J Therm Anal Calorim (2011) 103:163–170
DOI 10.1007/s10973-010-0894-6

Thermal properties of microcrystalline cellulose-filled PET–PTT blend polymer composites

Alper Kiziltas · Douglas J. Gardner · Yousoo Han · Han-Seung Yang

Received: 7 September 2009 / Accepted: 17 May 2010 / Published online: 30 June 2010

Abstract Polymer composite materials were prepared from poly(ethylene terephthalate)–poly(trimethylene terephthalate) blends as the matrix and different microcrystalline cellulose (MCC) filler levels (0–40 wt%) using melt compounding followed by compression molding. The composites were analyzed using dynamic mechanical thermal analysis (DMTA), differential scanning calorimetry (DSC) and thermogravimetric analysis (TG). The DSC results indicated that there is no consistent or significant influence of the MCC addition on the glass transition (T_g), melting (T_m), and crystallization temperature of the composites. With increasing MCC content, dynamic mechanical properties improved because of the reinforcing effect of the MCC. The tan δ peak values from the DMTA were not significantly changed as the MCC content increased. TG indicated that the onset temperature of rapid thermal degradation decreased with increasing MCC content. It was also found that the thermal stability of the composites slightly decreased as the MCC content increased.

Keywords Microcrystalline cellulose (MCC) · PET/PTT blends · Dynamic mechanical thermal analysis (DMTA) · Differential scanning calorimetry (DSC)

A. Kiziltas (✉) · D. J. Gardner · Y. Han · H.-S. Yang
AEWC Advanced Structures & Composites Center, University of Maine, Orono, ME 04469, USA
e-mail: alper.kiziltas@umit.maine.edu

A. Kiziltas
Department of Forest Industry Engineering, Faculty of Forestry, University of Bartin, 74100 Bartin, Turkey

Introduction

Cellulose is among the most abundant natural, renewable, and biodegradable materials in the world and can be obtained from many sources. It has been predicted that 10^{10} and 10^{11} tons of cellulose are produced and destroyed each year globally [1, 2]. Over the last few decades, interest in producing polymer composite materials with cellulose materials has received considerable attention [3–7]. Polymer composites with cellulose fibers are materials with unique properties compared to inorganic materials. The main advantages of cellulose is its renewable nature, high-specific strength and modulus (the elastic modulus for cellulose whiskers is about 145 GPa, while that of glass fibers averages about 70 GPa), low density ($\sim$1.6 g/cm^3 for cellulose and $\sim$2.5 g/cm^3 for glass fiber) compared to materials reinforced by inorganic substances, low-thermal conductivity, and the possibility of recycling. In addition, because of the non-biodegradability of most plastics, disposal is a significant challenge. As a solution, industrial and scientific research communities have shown great interest in blending plastic materials with natural biopolymers such as wood flour, cellulose, and starch [2, 6–9].

Synthetic and natural polymers are exposed to degradation under the effect of increased temperature. Therefore, it is extremely important to have information about the effect of the processing temperatures regarding processing duration because thermal stress can occur during the manufacturing of natural fiber reinforced composite materials with thermoplastic matrices [10]. Essential information regarding the thermal stability of natural and synthetic polymers can be obtained by thermal analysis, which is based on analytical experimental techniques that measure thermal behaviors and interfacial characteristics of composite materials as a function of temperature [10–12]. The

following techniques are often used for thermal analysis. Differential scanning calorimetry (DSC) can be used to determine melting temperature (T_m), glass transition temperature (T_g), crystallization temperature (T_c) and is also the easiest and most widely used thermal analysis technique in the world. Dynamic mechanical thermal analysis (DMTA) has become widely used and is an important technique for determining the viscoelastic properties of composite materials for purposes of investigating their dynamic material behavior such as storage modulus (E') and loss factor (tan δ) as a function of temperature. Thermogravimetric analysis (TG) can be used for determining the moisture content, thermal degradation temperature, and thermal stability of composite materials [11, 12].

Composite materials made from thermoplastic resins (polyethylene and polystyrene) and microcrystalline cellulose (MCC) have been studied [4, 13–15]. MCC is a purified, partially depolymerized cellulose, prepared by treating alpha-cellulose, obtained as a pulp from fibrous material with mineral acids, and it is used extensively in the manufacture of pharmaceuticals, food, paper, and composite materials [2]. The application of engineering thermoplastic polymer composites with MCC is limited by the lack of information about morpho-structural aspects and the behavior of such materials when mechanical and thermal stresses are applied. Aromatic polyesters, including poly(ethylene terephthalate) (PET) and poly(trimethylene terephthalate) (PTT), are polyester high-performance engineering plastics used in manufacturing and are widely used in many areas including the textile, electronics, automotive industries, etc. [16–21]. In recent years, many researchers have been interested in blends or copolymers to increase the crystallization rate of PET or to improve the mechanical and thermal properties of PTT [16–21]. In the present study, PTT was used to reduce the processing temperature and increase the crystallization rate of PET [16]. Liang et al. found that PET–PTT blends showed a single composition-dependent glass transition temperature and cold crystallization peak over all compositions, suggesting that PET and PTT were miscible in the amorphous state. Polymer miscibility of blends is determined by measuring their glass transition temperature (T_g) from DSC scans. In general, for immiscible blends, two or more T_gs generally appear in a DSC scan indicating phase separation, whereas for miscible blends or copolymers only one T_g is observed in the amorphous phase [16].

The aim of this study was to investigate the effect of MCC on the thermal properties of the PET–PTT composites. MCC was incorporated over a content ranging from 0 to 40 wt%. In the present study, PET–PTT-based composites were prepared with MCC as the filler phase by thermal mixing followed by compression molding.

Experimental procedure

Materials

The PET and PTT were supplied as polymer pellets by Shell Co. and Azom Co., USA, respectively. The PET and PTT had densities of 1.3–1.4 and 1.35 g/cm^3, and melt flow indices of 0.65 and 0.92 dl/g, respectively. The 2:1 PET to PTT blending ratio was selected based on our previous observations that PET–PTT blend at this ratio showed better mechanical and thermal properties in comparison with their other formulations. The lubricant (TPW 113), used as an additive to improve processing conditions, was supplied by Struktol Co. The MCC used as the reinforcement was a powder with a particle size range from 26 to 96 μm. The average particle size was 50 μm. The MCC is highly crystalline cellulose supplied by Sigma-Aldrich Co. The MCC was stored in sealed containers after being oven dried for at least 16 h at 105 °C to obtain low moisture content of less than 1%.

Sample preparation

The MCC, PET, and PTT were dried using an oven set at 105 °C for 16 h until the moisture content was less than 1%. The matrix polymer PET–PTT blends were mixed with the MCC. The compounding was conducted using a Brabender Prep-mixer® equipped with a bowl mixer and the process temperature and torque changes were measured in real time. Melt temperature and torque changes for every run were recorded to determine optimum processability for the PET–PTT blend–MCC composites. The basic processing parameters are listed in Table 1. The mixer temperature was set to 270 °C, and the polymer melt

Table 1 Basic operating parameters of the brabender rheomixer for PET/PTT blends

Stage level	Operating parameters				
	Set temp.	Melt temp.	RPM	Mix melt temp.	Reaction time/min
First stage/PET–PTT	270	260	60–70	–	7
Second stage/with MCC	230	200–230	50	Cont. under 230	3

Table 2 Composition of PET–PTT polymer composites

Sample code	Composition			
	MCC contents	PET	PTT	Lubricant
Neat PET/PTT	0	63	32	5
PET/PTT–MCC2.5	2.5	61.5	31	5
PET/PTT–MCC5	5	60	30	5
PET/PTT–MCC10	10	56.5	28.5	5
PET/PTT–MCC20	20	50	25	5
PET/PTT–MCC30	30	43	22	5
PET/PTT–MCC40	40	37	18	5

Values are in wt%

temperature decreased to 230 °C where the polymer blend appeared to experience good melting. The revolutions per minute (RPM) of the mix blades were increased from 60 to 70 so that the generated shear might facilitate polymer melting. MCC was added to the mixer when the polymer melt appeared well mixed. After addition of the MCC, the melt temperature dropped sharply to 200 °C and increased again as the mixing progressed. The melt mixture was released from the mixture immediately after the temperature reached 230 °C. These temperature ranges and MCC residence times were recognized as a relatively safe temperature range to prevent severe thermal degradation with a guarantee of composite processability. The PET–PTT blend and MCC-filled compounds were granulated using a lab scale grinder. The ground particles were dried in an oven at 105 °C for 16 h and placed on a steel mold heated up at 230 °C. The mold was compressed at 60 tons for 5 min using a $2' \times 2'$ hot press and then cooled at the same pressure before release from the mold in 30 min. Then the compressed panel samples were conditioned at 25 °C and 50% R.H. for 48 h prior to the thermal tests. The compositions are shown in Table 2.

Thermal properties

Differential scanning calorimetry (DSC)

Differential scanning calorimetry analysis was carried out using a Perkin Elmer Instrument Pyris DSC with a sample weight of 8 to 10 mg. All samples were held at 30 °C for 5 min, heated at a rate of 20 °C/min to 300 °C, subsequently held for 5 min to erase the previous thermal history, then cooled at a rate of 20 °C/min to 30 °C, subsequently held for 5 min and heated again at a rate of 20 °C/min to 300 °C under a nitrogen atmosphere. The glass transition, cold crystallization, and melting temperatures were determined from the second heating scan. The T_g was taken from the second heating scan as the inflection point of the specific heat increment at the glass–rubber transition. The T_m value was taken as the maximum of the endothermic melting peak in the second heating. At least three randomly picked samples from ground samples were tested for each composition and the results are presented as an average for tested samples.

Dynamic mechanical thermal analysis (DMTA)

The viscoelastic properties of the composites were determined using a Rheometric Scientific DMTA IV. The experiments were conducted in three point bending mode under isochronal conditions at a frequency of 1 Hz. The strain amplitude was fixed at 0.01% to be in the domain of the linear viscoelasticity of the composites. The composite materials were sawn into small strips on a vertical milling machine using a 1.45 mm × 75 mm, 36 tooth blade, attached to an arbor. The samples were cut in a rectangular shape with dimensions about 42 mm × 3.2 mm × 1.8 mm. The temperature range was from −50 to 150 °C at a scanning rate of 3 °C/min. The storage modulus (E'), loss modulus (E''), and loss factor (tan δ) of the samples were measured as a function of temperature. At least three samples were tested for each composition and the results are presented as an average for tested samples.

Thermogravimetric analysis (TG)

Thermogravimetric analysis measurements were carried out using a Mettler Toledo analyzer on samples of about 10 mg. Each sample was scanned over a temperature range from room temperature to 600 °C at heating rate of 10 °C/min under nitrogen with a flow rate 20 mL/min to avoid sample oxidation. The five individual samples used for the TG measurement were randomly selected from ground samples.

Results and discussion

Differential scanning calorimetry (DSC)

The effect of the MCC on the thermal properties of the thermoplastic polymer composites was examined in non-isothermal DSC experiments. The values of glass transition temperature (T_g), melting temperature (T_m), crystallization temperature (T_c), and corresponding melting enthalpies (ΔH_m) and crystallization enthalpies (ΔH_c) are presented in Table 3. The glass transition temperature provides important evidence for blend miscibility. If the blend is one phase, only one glass transition temperature is evident, and it could be concluded that two different polymers were miscible. If the blend is two phases, two glass transition temperatures are evident and it can be concluded that the

Table 3 Summary of T_g, T_m, T_c, ΔH_m (J/g), and ΔH_c for the MCC-filled PET–PTT composites

Sample Code	T_g/°C	T_m/°C	T_c/°C	ΔH_m/J/g	ΔH_c/J/g
Neat PET–PTT	68.1 (0.1)	249.2 (0.2)	186.6 (2.6)	37.1 (1.4)	−52.2 (2.7)
PET–PTT–MCC2.5	68.4 (0.7)	244.9 (0.1)	186.3 (0.7)	34.9 (0.4)	−51.7 (1.1)
PET–PTT–MCC5	68.1 (1.1)	247.5 (0.5)	182.8 (0.2)	33.4 (0.5)	−49.2 (2.5)
PET–PTT–MCC10	68.3 (0.7)	248.1 (0.9)	183.8 (0.9)	31.9 (1.1)	−47.8 (1.7)
PET–PTT–MCC20	67.2 (0.2)	248.6 (0.9)	192.3 (0.9)	28.9 (1.5)	−44.9 (1.9)
PET–PTT–MCC30	66.4 (0.5)	249.3 (1.8)	194.4 (1.1)	26.6 (1.1)	−41.8 1.6)
PET–PTT–MCC40	67.9 (1.4)	249.6 (1.1)	195.3 (0.4)	21.4 (0.5)	−35.7 (2.2)

Parenthesis indicates standard deviation. ΔH_m is calculated based on total area of endothermic peak

blend is not miscible [16]. In Fig. 1, all composites showed only one T_g value and the T_g values of composites are between 65 and 70 °C and as MCC loading increased, the T_g of the composites changed, but only marginally in Fig. 1. Another evidence for miscibility is cold crystallization [16]. Figure 2 showed only one cold crystallization temperature, which is between 125 and 135 °C for all composites. The single T_g and cold crystallization temperature shows that the PET–PTT blend and composites are compatible in the amorphous phase. This implies that no chemical bonding occurs at the interface between the matrix polymer and MCC. In other words, the MCC is physically encapsulated by the melted matrix polymer and physically inhibits the mobilization of the polymer chain. If interfacial adhesion such as chemical bonding were to occur between the matrix polymer and MCC, the T_g of the thermoplastic polymer composites would be substantially changed compared with that of the neat PET–PTT blends [16, 17, 21]. The PET–PTT blend and MCC-filled composites displayed similar thermograms and small differences in their melting temperatures were within the experimental precision of the equipment. The melting point was taken as the main peak of the endothermic curve. Dual melting peaks can be observed from all composites in Fig. 3. Due to melting peaks associated with the destruction of the crystalline region of the polymer blend, the two melting peaks suggest that the chain segments of PET and PTT tend to crystallize in their crystal phase [21]. The larger melting peak is associated with the PET because of its higher content in the composite blend. It can be seen for Fig. 3 that the melting point of PET and PTT is about 250 and 225 °C, respectively, and the melting points of

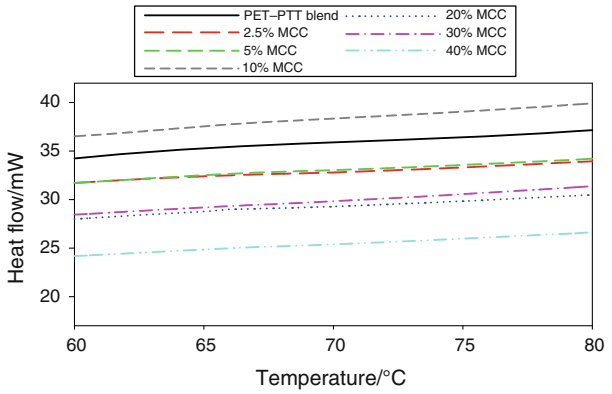

Fig. 1 Glass transition temperatures from DSC for PET–PTT blend and MCC-filled PET–PTT composites at different filler loadings

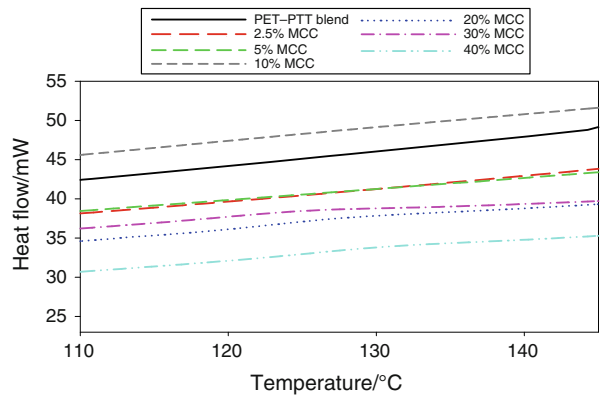

Fig. 2 Cold crystallization temperatures from DSC for PET–PTT blend and MCC-filled PET–PTT composites at different filler loadings

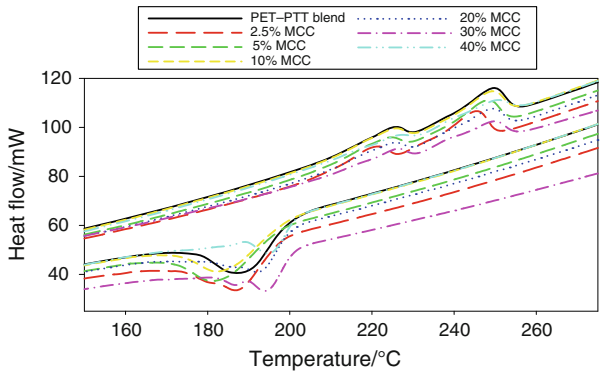

Fig. 3 The effect of MCC loading on the melting and crystallization temperatures for the PET–PTT blend and MCC-filled PET–PTT composites at different filler loadings

composites are between 244 and 250 °C. There is no consistent or significant influence of the MCC addition on the melting temperature. From these results, it can be concluded that the T_g and T_m values of the composites were strongly influenced by the matrix polymer. Furthermore, the T_m of the composites plays an important role in determining their processing temperature and thermal properties [11, 12]. Figure 3 shows the T_c of PET–PTT blend and composites. Figure 3 illustrates that adding MCC addition does not change the crystallization temperature of the composites or it has a slight effect at most. However, increasing MCC content, in all cases, results in lower temperature of crystallization enthalpies (ΔH_c) and melting enthalpies (ΔH_m) in Table 3.

Dynamic mechanical thermal analysis (DMTA)

Figure 4 shows the temperature dependence of the storage modulus and loss factor (tan δ) of PET–PTT blend and MCC-filled composites. The PET–PTT blend shows typical behavior for a semi-crystalline polymer with three distinct regions that could be identified as glassy, glass transition, and rubbery regions. In the glassy region (temperature is below 30 °C), the storage modulus (E') remains roughly constant. Around 35 °C, the modulus decrease is related to the glass transition region of the PET–PTT blend amorphous phase. The magnitude of this storage modulus decrease is small due to high degree of crystallinity of the blend. At higher temperatures after the glassy region (temperature is higher than 30 °C), the storage modulus decreases sharply because of the increased viscosity and polymer chain mobility [11, 12, 22]. The sharp decrease in the storage modulus is continued until the rubbery region is reached. MCC-filled composites show a similar behavior and have a higher modulus for all temperature ranges compared to the unfilled composites. The higher modulus for the composites could be a result of the high degree of crystallinity of the PET–PTT blend in the composite formulations, but DSC measurements show that the degree of crystallinity of the PET–PTT blend was composition-independent up to 30 wt% MCC, and then decreases for a high loading of MCC [22]. We can assume that the increase in the composite modulus should be related to the reinforcing effect of MCC. A similar observation was reported for semi-crystalline poly(caprolactone) reinforced with chitin whiskers and poly(oxyetylene) reinforced with cellulose nanocrystals [22, 23]. Also, it can be seen from Fig. 4 that the composites with MCC exhibit much better temperature stability than the PET–PTT blend in the rubbery region due to the percolating network effect [24]. Figure 5 shows that the storage modulus of the composites increased with increasing MCC percent at room (25 °C) and glass transition (90 °C) temperature. At 40 wt% MCC loading, the storage modulus increased significantly. As the MCC loading increases, the stress is more evenly distributed throughout the composite and therefore the modulus increases with the addition of MCC compared to the

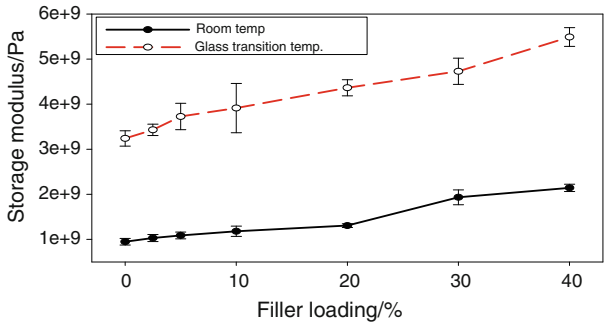

Fig. 5 The storage modulus of PET–PTT blend and MCC-filled PET–PTT composites at the room temperature and glass transition temperature

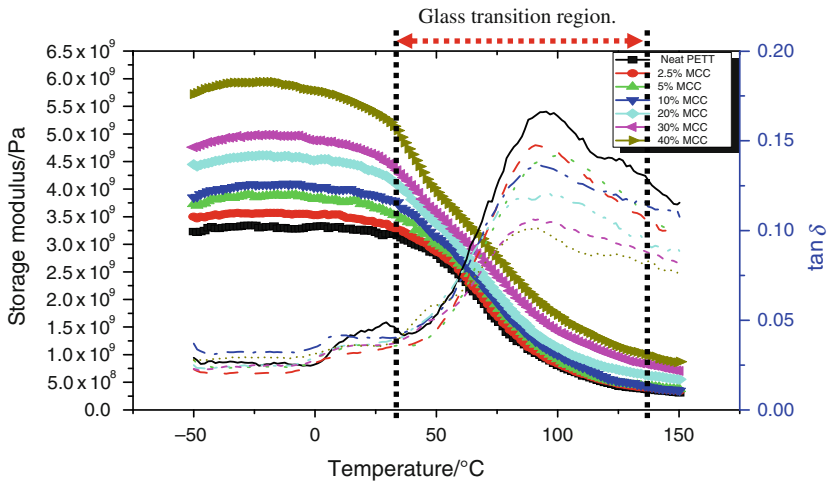

Fig. 4 Storage modulus and loss factor (tan δ) of PET–PTT blend and MCC-filled PET–PTT composites from −50 to 150 °C as a function of temperature

PET–PTT blend. In addition, strong interactions, which arise from the hydrogen bonds between cellulose molecules and fibers and fibrils, lead to much a greater storage modulus [24].

The temperature dependence of tan δ versus the MCC-filled PET–PTT composites as a function of temperature at a frequency of 1 Hz is presented in Fig. 4. The shift in tan δ peak temperature provides information about molecular interactions between the PET–PTT blend and MCC [24]. From the peak in the tan δ curve, we can see that the incorporation of MCC has no consistent or significant influence on the glass transition temperature of the composite, but it does have a significant effect on the magnitude of tan δ values. The tan δ_{max} peak values correspond to the glass transition temperature and these values are not significantly changed as the MCC content is increased because the viscoelastic properties of the composite are strongly influenced by the matrix polymer. Figure 4 indicates that the tan δ peak did not exhibit any shift, which indicates that there are no molecular interactions between the polymer matrix and MCC. As a result, we can see that the reinforcing effect is related mainly to the cellulose network and the strong interaction of the cellulose particles [11, 12, 24]. The neat PET–PTT blend presents a tan δ peak temperature of about 95 °C and the composites present tan δ peak temperatures between 86 and 95 °C. On the other hand, the difference in the tan δ values between the neat PET–PTT blend and the composites at low temperature is only marginal. At higher temperatures, however, this difference is more prominant. The magnitude of tan δ peak values of MCC-filled composites was significantly decreased around the glass transition temperature in Fig. 4, because of the restriction in the chain segment mobility in the amorphous region of the PET–PTT blend brought about by the incorporation of MCC [11]. Below glass transition temperature, which is sometimes referred to as the α transition, β relaxation observed for all composite materials at around 20–30 °C. The β relaxation is normally attributed to polymer backbone conformation reorganization and it related to the amorphous region [25].

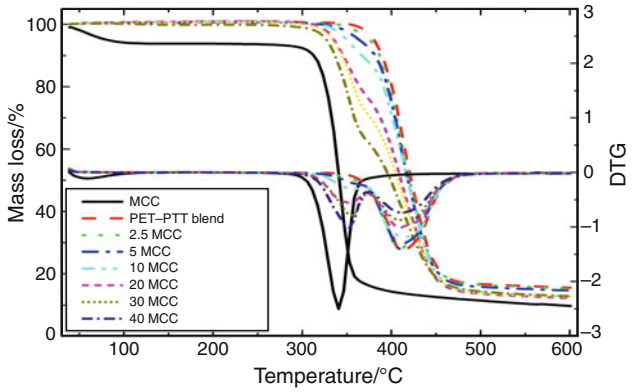

Fig. 6 TG and DTG curves of PET–PTT blend and MCC-filled PET–PTT composites

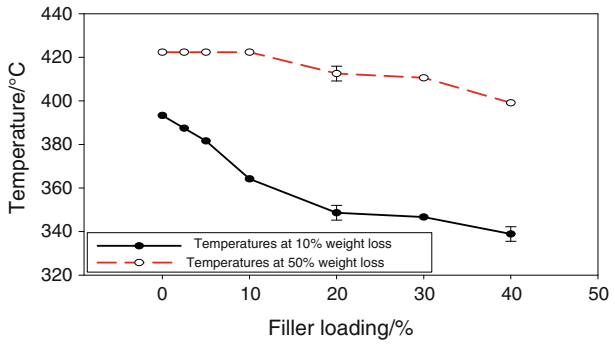

Fig. 7 Temperatures at 10 and 50% mass loss for PET–PTT blend and MCC-filled PET–PTT composites

Thermogravimetric analysis (TG)

The TG and DTG curves for PET–PTT blend and MCC-filled composites are shown in Fig. 6. The degradation

Table 4 Thermogravimetric data for PET–PTT blend and MCC-filled PET–PTT composites

Sample Code	DTG temperature/°C		M.L./%		Residue/%	M.L at 600 °C
MCC	341.7 (1.2)		52.2 (0.7)		9.7 (0.8)	84.5 (0.8)
PET–PTT Blend	410.8 (0.2)		33.7 (1.1)		15.5 (0.8)	84.5 (0.8)
PET–PTT–MCC2.5	410.8 (0.2)		37.0 (1.7)		15.2 (0.7)	85.8 (0.7)
	First peak	Second peak	First peak	Second peak		
PET–PTT–MCC5	369.3 (0.5)	410.8 (0.2)	6.4 (0.4)	39.5 (0.2)	14.6 (0.2)	85.4 (0.2)
PET–PTT–MCC10	358.4 (0.6)	409.8 (1.6)	9.3 (0.2)	41.0 (0.1)	12.7 (0.3)	87.3 (0.3)
PET–PTT–MCC20	352.3 (2.1)	408.8 (2.2)	17.0 (2.1)	50.7 (2.5)	12.1 (0.7)	87.9 (0.7)
PET–PTT–MCC30	353.3 (0.5)	410.8 (0.0)	20.6 (0.5)	52.0 (1.2)	12.6 (0.1)	87.4 (0.1)
PET–PTT–MCC40	352.5 (0.5)	410.8 (0.2)	24.1 (0.3)	58.3 (0.3)	12.8 (0.3)	87.2 (0.3)

Parenthesis indicates standard deviation

temperatures of the PET–PTT blend and MCC-filled composites are different. The PET–PTT blend and 2.5% MCC-filled composites undergo a single-stage degradation with a single peak at 410 °C, whereas high MCC-filled composites show two degradation peaks in the range 340–415 °C. The temperature at 10% mass loss (T_{10}) and the temperature at 50% mass loss (T_{50}) for the neat PET–PTT blend and MCC-filled composites are shown Fig. 7. Both T_{10} and T_{50} values for the composites decreased monotonically from the PET–PTT blend to 40 wt% MCC addition. It is obvious from Table 4 that the percentage of mass loss for composites increased from around 84% for the neat PET–PTT blend to 87% for 20 wt% MCC addition. Beyond the 20 wt% MCC addition, mass loss in the composites decreased. The results also show that as the filler loading increased, the thermal stability of the composites slightly decreased as the MCC content increased because of the lower thermal stability of MCC compared to the PET–PTT blend. A summary of mass loss (%), peak temperature, and mass loss after 600 °C of the composites are given in Table 4.

Conclusions

MCC-filled PET–PTT blend composites were prepared by melt compounding followed by compression molding. There is no consistent or significant influence of the MCC addition on the glass transition (T_g) or melting (T_m) and crystallization (T_c) temperatures of the composites. The storage modulus of the MCC-filled PET–PTT composite system was higher than that of the neat PET–PTT blend and increased with increasing MCC content. This was attributed to the reinforcement effect of the MCC, and this reinforcing effect is related mainly to the cellulose network and strong interaction among cellulose particles. MCC has also no significant influence on the tan δ peak temperatures as the MCC content is increased because the viscoelastic properties of the composite were strongly influenced by the matrix polymer. TG indicated that the MCC did not show significant initial degradation under 300 °C. Therefore, MCC-filled composites could be used for high temperature circumstances, such as in the automobile industry. It is believed that the formulation containing only PET/PTT blend and MCC (without lubricant) will show better storage modulus and thermal stability and less change in the melt behavior of composites in comparison with lubricant added PET/PTT blend and MCC formulation. In this study, lubricant used only as an additive to improve processing conditions.

Acknowledgements The Republic of Turkey, Ministry of National Education is greatly acknowledged for support of the scholarship of the researcher Alper Kiziltas to do this study at the University of Maine. The authors thank Chris West for the sample preparation. The authors would also like to thank Maine Agricultural and Forest Experiment Station (MAFES) project ME09615-08MS and the Wood Utilization Research Hatch 2007–2008 project. This is the 3069th paper of the Maine Agricultural and Forest Experiment Station.

References

1. Helbert W, Cavaillé JY, Dufresne A. Thermoplastic nanocomposites filled with wheat straw cellulose whiskers. Part I: processing and mechanical behavior. Polym Compos. 1996;17(4):604–11.
2. Azizi Samir MAS, Alloin F, Dufresne A. Review of recent research into cellulosic whiskers, their properties and their application in nanocomposite field. Biomacromolecules. 2005;6(2):612–26.
3. Petersson L, Kvien I, Oksman K. Structure and thermal properties of poly(lactic acid)/cellulose whiskers nanocomposite materials. Compos Sci Technol. 2007;67(11–12):2535–44.
4. Panaitescu DM, Notingher PV, Ghiurea M, Ciuprina F, Paven H, Iorga M, Florea D. Properties of composite materials from polyethylene and cellulose microfibrils. J Optoelectron Adv Mater. 2007;9(8):2524–8.
5. Bondeson D, Kvien I, Oksman K. Strategies for preparation of cellulose whiskers from microcrystalline cellulose as reinforcement in nanocomposites. Am Chem Soc (ACS symposium series; 938);2006:10–25.
6. Goodrich JD. The utilization of cellulose and chitin nanoparticles in biodegradable and/or biobased thermoplastic nanocomposites. PhD dissertation, State University of New York College of Environmental Science and Forestry, Syracuse, New York, U.S.; 2007.
7. Panaitescu DM, Donescu D, Bercu C, Vuluga DM, Iorga M, Ghiurea M. Polymer composites with cellulose microfibrils. Polym Eng Sci. 2007;47(8):1228–34.
8. Sturcova A, Davies GR, Eichhorn SJ. Elastic modulus and stress-transfer properties of tunicate cellulose whiskers. Biomacromolecules. 2005;6(2):1055–61.
9. Eichhorn SJ, Baillie CA, Zafeiropoulos N, Mwaikambo LY, Ansell MP, Dufrense A, Entwistle KM, Herrera-Franco PJ, Escamilla GC, Groom L, Hughes M, Hill C, Rials TG, Wild PM. Review current international research into cellulosic fibers and composites. J Mater Sci. 2001;36:2107–31.
10. Wielage B, Lampke T, Marx G, Nestler K, Starke D. Thermogravimetric and differential scanning calorimetric analysis of natural fibres and polypropylene. Thermochim Acta. 1999;337(1–2):169–77.
11. Kim H-S, Kim S, Kim H-J, Yang H-S. Thermal properties of bio-flour-filled polyolefin composites with different compatibilizing agent type and content. Thermochim Acta. 2006;451(2):181–8.
12. Kim H-S, Yang H-S, Kim H-J, Lee B-J, Hwang T-S. Thermal properties of agro-flour-filled biodegradable polymer bio-composites. J Therm Anal Calorim. 2005;81(2):299–306.
13. Laka MG, Chernyavskaya SA. Physicomechanical properties of composites containing Thermocell microcrystalline cellulose as filler. Mech Compos Mater. 1996;32(4):381–6.
14. Maskavs A, Kalnins M, Laka M, Chernyavskaya S. Physicomechanical properties of composites based on low-density polyethylene and cellulose-containing filers. Mech Compos Mater. 2001;37(2):159–66.
15. Maskavs M, Kalnins M, Reihmane S, Laka M, Chernyavskaya S. Effect of water sorption of some mechanical parameters of composite systems based on low-density polyethylene and

microcrystalline cellulose. Mech Compos Mater. 1999;35(1): 55–62.
16. Liang H, Xie F, Chen B, Guo F, Jin Z, Luo F. Miscibility and melting behavior of poly(ethylene terephthalate)/poly(trimethylene terephthalate) blends. J Appl Polym Sci. 2007;107(1):431–7.
17. Liang H, Xie F, Guo F, Chen B, Luo F, Jin Z. Non-isothermal crystallization behavior of poly(ethylene terephthalate)/poly(trimethylene terephthalate) blends. Polym Bull. 2008;60:115–27.
18. Wei G, Wang L, Chen G, Gu L. Synthesis and characterization of poly (ethylene-co-trimethylene terephthalates). J Appl Polym Sci. 2005;100(2):1511–21.
19. Son TW, Kim KI, Kim NH, Jeong MG, Kim YH. Thermal properties of poly(trimethylene terephthalate)/poly(ethylene terephthalate) melt blends. Fiber Polym. 2003;4(1):20–6.
20. Chen X, Yang K, Gong H, Chen Y, Dong Y, Liao Z. Crystallization behavior and crystal structure of poly(ethylene-co-trimethylene terephthalates). J Appl Polym Sci. 2007;105(5): 3069–76.
21. Ge Q, Ding X, Wu G, Liang S, Wu S. Study on the microstructure and mechanical properties of PET and PET/PTT Blends. Key Eng Mater. 2007;340–341:1085–90.
22. Azizi Samir MAS, Alloin F, Sanchez J-Y, Dufresne A. Cellulose nanocrystals reinforced poly(oxyethylene). Polymer. 2004;45(12): 4149–57.
23. Morin A, Dufresne A. Nanocomposites of chitin whiskers from riftia tubes and poly(caprolactone). Macromolecules. 2002; 35(6):2190–9.
24. Seydibeyoglu MO, Oksman K. Novel nanocomposites based on polyurethane and micro fibrillated cellulose. Compos Sci Technol. 2008;68:908–14.
25. Perkin Elmer, Thermal Anlaysis, Application Note. Waltham, MA: Perkin Elmer Inc.